Hindawi

Research Article

Arc-Scanning Synthetic Aperture Radar for Accurate Location of Targets

Félix Pérez-Martínez,[1] **Susan Martínez-Cordero,**[1] **Jaime Calvo-Gallego** [ID]**,**[2] **and Francisco-Javier Romero-Paisano**[1]

[1]*Microwave and Radar Group, Information Processing and Telecommunications Center,*
Escuela Técnica Superior de Ingenieros de Telecomunicación, Universidad Politécnica de Madrid, Madrid 28040, Spain
[2]*Department of Computing and Automatics, University of Salamanca, Zamora, Spain*

Correspondence should be addressed to Jaime Calvo-Gallego; jaime.calvo@usal.es

The purpose of this article is to present the advantages that the use of arc-scanning synthetic aperture radar (Arc-SAR) would provide for accurate location of target to the weapon systems. Arc-SAR systems have an extraordinary capacity of angular discrimination of the targets, this fact make possible they can be used for the precise location of targets by replacing the large antennas required by the monopulse systems, used in this kind of applications, with a small rotating antenna. However, to carry out the real-time location of targets with the current processors a much more complex signal processing is needed. A simulator has been developed in this work, which allows the comparison of the theoretical and experimental results obtained by the classical systems against those obtained with the proposed Arc-SAR system working in the millimeter frequency bands. The results obtained demonstrate the ability of the proposed technique to accurately locate targets. This confirms that the obtained precisions allow the use the presented system in some important applications as Sense & Avoid (S&A) and weapon-pointing systems. Finally, possible applications of these techniques are described, especially useful is onboard sensors, because of the small size and weight of the antenna needed to implement an Arc-SAR system.

1. Introduction

The monopulse systems [1] are a classic radio direction-finding technique used, among other fields, in radar systems for the accurate measurement of the direction of targets, both in surveillance radars for the detection and approximate location of targets, and in tracking radars for targeting systems for weapon aiming.

Synthetic aperture radar (SAR) is a high-resolution 2-D imaging radar system that uses the movement of the platform to synthesize a virtual large-aperture array antenna to achieve high-resolution imaging in the azimuth. SAR is a technology very mature [2]. Arc-SAR is a special SAR, working in a strip mode but with a circular aperture that has a 360° omnidirectional observation capability. The radiating system is on ground or on stationary aerial platform and follows a circular path at uniform angular velocity, transmitting and receiving signals in the direction perpendicular to the movement. The technique is

used to obtain images because of the extraordinary capacity they have in the angular discrimination of targets when large apertures are synthesized in terms of the wavelengths of the transmitted signal. A complete description of this technique can be found in [3].

Arc-SAR was proposed by Klausing et al. [4, 5]. They were the first to propose a SAR capable of taking advantage of the rotating movement of a helicopter blades to synthesize a large aperture. In the following years, numerous works were published in order to validate the technique, optimize the processing algorithms, and describe some applications, aimed at obtaining 3D topographic images, measurements of ground deformation or the location of objects on a surface [6–16].

On the other hand, in radar systems, angular discrimination and angular accuracy characteristics are associated. So, as it is proposed in this paper, it is possible to use Arc-SAR for the accurate localization of targets, replacing the large

antennas required by the monopulse systems with a small rotating antenna. The small size and weight of the antenna facilitate its installation on aerial platforms, especially if the platform has the ability to move circularly or incorporates mobile elements with this type of movement (helicopters, quadcopters, etc.). Similar systems for the different applications have been reported in some works. In [15], an Arc-SAR for airport runway foreign object debris detection. A similar detection system had already been proposed in [6]. Likewise, in [8] the same concept is presented for robot navigation by scanning the environment and detecting obstacles by means of a short-range synthetic aperture rotating radar.

In this document, after briefly describing the structure and main characteristics of the two types of systems, the results of the computer simulations of both systems working under similar conditions, are presented. After that, in order to validate the simulated a prototype of Arc-SAR radar working in the millimeter bands developed by the microwave and radar group (GMR), of the Information Processing and Telecommunications Center of the Escuela Técnica Superior de Ingenieros de Telecomunicación of the Universidad Politécnica de Madrid (ETSIT-UPM), is presented. Later, the experimental characterization of the prototype is summarized, where the possibilities of the proposed technique are confirmed [17]. Finally, some conclusions in which some applications where the advantages provided by these systems can be exploited are presented.

2. Monopulse Systems

In a radar that uses the monopulse technique, the echoes of the targets are received by an antenna system composed in each plane by two slightly off-centered lobes. The outputs of each antenna are combined to obtain the sum and difference radiation diagrams (Σ and Δ) that are carried to a "monopulse processor" that establishes the ratio Δ/Σ from which the angle of incidence is extracted. Obviously, four lobes are required to obtain the direction of a target, two in the azimuth plane and two in the elevation plane, although in some applications only one plane is required. It is a well-known system and frequently used so we will not insist on its description [1].

A characteristic to highlight is that main features (angular resolution (angular resolution is defined as the ability to resolve two targets located at the same distance.), $\Delta\theta$, and angular precision (angular precision is the error in measuring the direction of a target and is quantified by the standard deviation of a zero-mean Gaussian distribution.), σ_θ), basically, depend on the shape of the radiation diagrams Δ and Σ. It can be estimated from the following expressions [18]:

$$\Delta\theta \approx \theta_B \, \sigma_\theta \approx \frac{\theta_B}{K_m \cdot \sqrt{2 \cdot \text{SNR}}} \approx \frac{0.44 \cdot \theta_B}{\sqrt{\text{SNR}}}, \qquad (1)$$

where θ_B is the beam width at 3 dB of the sum diagram, K_m is the slope of Δ/Σ ($1.2 < K_m < 2$), and SNR is the signal-to-noise ratio produced by the received echo. In this work we have taken a typical value of $K_m = 1.6$ [19]. As on the other hand,

$$\theta_B = \frac{K \cdot \lambda}{L_{\text{ap}}}, \qquad (2)$$

where K is the aperture efficiency of the antenna ($0.7 < K < 0.9$), λ the wavelength of the transmitted signal, and L_{ap} is the physical length of the antenna. It is immediate to obtain that the performance of monopulse systems is associated with the size of the antennas, expressed in terms of wavelengths (electrical aperture), we have taken the intermediate value for K ($K = 0.8$) as follows:

$$\Delta\theta \approx \frac{K \cdot \lambda}{L_{\text{ap}}} \, \sigma_\theta \approx \frac{0.35 \cdot \lambda}{L_{\text{ap}} \cdot \sqrt{\text{SNR}}}. \qquad (3)$$

Note that theoretically, the error is zero if the echo comes with a very high SNR, which in practice is not true because the imperfections of the circuitry that produce a minimum instrumental error of the order of 20 times less than the beam width θ_B. The formula assumes (as it is done in the practical cases) that the angle is established by averaging the measurements obtained for the two echoes closest to the axis of the antenna.

3. Arc-SAR Systems

As already described, an Arc-SAR system is basically, an SAR system in which a circular aperture is synthesized. In SAR systems in order to obtain high resolution in the direction perpendicular to the trajectory of the aerial platform (called slant-range resolution); it is necessary to transmit signals of great bandwidth. On the other hand, to achieve high resolution in the direction parallel to the trajectory of movement of the aerial platform (called cross-range resolution, if it is expressed as a length, $\Delta x = R \cdot \Delta\theta$, where R is the distance to the target), we must increase the angle with which the scene is observed. In this way, we can synthesize an aperture equivalent to a larger antenna and therefore more directive.

When the aperture is circular and the target is in the same plane as the movement of the antenna, the estimated angular resolution is given by Klausing and Keydel [5] as follows:

$$\Delta\theta \approx \frac{\lambda}{5 \cdot L \cdot \sin\frac{\alpha}{2}}, \qquad (4)$$

where L is the rotation radius of the antenna and α is the angle scanned by the antenna. Note that the expression does not depend on the size of the antenna and that excellent angular resolutions can be achieved, and therefore very high-angular accuracies, if the electric aperture is high.

Numerous algorithms have been proposed to extract the distance–angle images (in a plane) and to segment the targets whose centroids allow the establishment of their corresponding distance and angle. The calculation or estimation of the angular error is much more complicated in this case, since it depends on the signal process used, which is why its
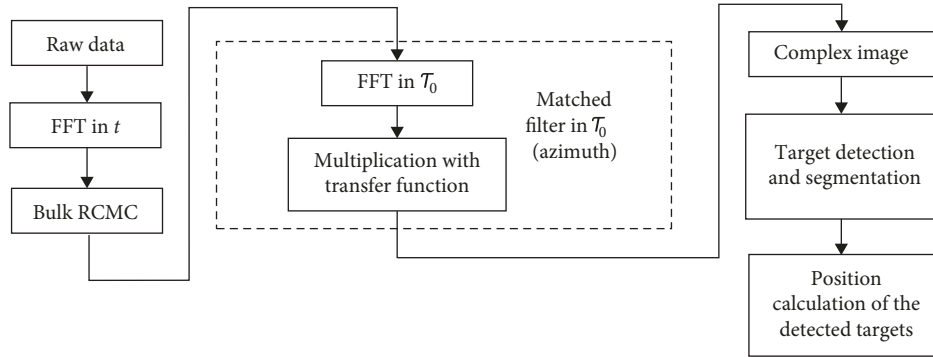
FIGURE 1: Block diagram of the back-projection algorithm.

simulation has been used with the simulator developed by a GMR research group of an ETSIT-UPM.

For the purposes of this work, a radar that works with continuous wave signals and modulated frequency and the azimuthal processing known as the back projection algorithm (BPA) has been selected [7] BPA is a time-domain algorithm, which has the advantages of presenting good image quality, high precision and adaptation to any radar geometry, although they have the disadvantage of the computational complexity for real-time image processing. Figure 1 shows the specific processes of one of the developed algorithms, which is used in this work.

The signal processing performs a fast Fourier transform (FFT) weighted with the raw data ($I + jQ$) that is obtained at the radar receiver output, in the fast time domain, t, thereby compressing the image in radial range.

After that, the migration of cells in distance is corrected by a process known as range cell migration correction (RCMC), so that it is possible to compute the signal processing in azimuth (transverse range or azimuth) of all the cells of the same radial range. Azimuthal migration of cells is not corrected.

Then the correlation of the signal, with respect to the long time variable, τ_n, is performed with the reference function, to compress the image in azimuth. This correlation is implemented by multiplying the FFT of an image with respect to τ_n, by the FFT of the reference function, and performing the inverse FFT (IFFT), again, with respect to τ_n, of the result of the mentioned multiplication.

The segmentation process used is by similarity, with a thresholding criterion. Based on a constant false alarm rate (CFAR) technique, the image is divided into its constituent parts, in order to isolate the regions of interest from the rest of the image, looking for regions that have similar values, and then, through a process of binarization, an object is distinguished from the background of the image.

After segmenting the image, we proceed to extract the regions that it contains, labeling all the related components (cells whose value is "1" and are connected to each other by a set of cells with value "1"), giving as result a region.

To carry out the labeling of the connected components in a binary image, that is, the segments found in the range/azimuth matrix, the "Flood-Fill" algorithm is used [20], which determines the area formed by the contiguous elements in a multidimensional matrix. The "Flood-Fill" algorithm works by filling or recoloring a specific area that contains different colors from the inside to the edge of the image. This algorithm can use connectivity-4 neighbors or connectivity-8 neighbors, to determine the regions and classify them, in this case with different color.

Finally, to obtain the location of the captured targets, assuming each region as a target, we calculate the center of mass or centroid, obtaining distance and azimuth information for each target.

4. Simulation Results

The simulation program developed allows the definition and analysis of any three-dimensional scenario with several point targets that are characterized by their radar section. It consists of two software programs. In the first one, the antennas are modeled and the total signal received in the radar from the targets is calculated during the circular exploration of the antennas. While, in the second one, thermal noise can be added, defined in terms of SNR at the receiver input, and all the signal and data processes incorporated by the radar are strictly reproduced, adding in its case, some imperfections whose effect you want to analyze.

The software programs, developed in MATLAB™, allow to obtain numerous intermediate results, and include the possibility of feeding it real data. In the main interface of the simulator, the input data of the scenario to be simulated can be configured, such as: maximum distance, minimum distance, angular speed, radius of gyration (L), modulating signal frequency (f_m), sampling frequency (f_s), initial sweep angle, angle sweep (for scanning), and radar module configuration, for example, 0° (antennas in horizontal position for radiation pattern in azimuth of 12° and elevation 80°) and 90° (antennas in vertical position for radiation pattern in azimuth of 80° and elevation 12°).

Figures 2 and 3 show the user interface and some of the results of the software programs when the scenario that will later be used to experimentally characterize the developed prototype is introduced.

Using the developed software tool, several parametric analyses of the system have been carried out in order to select the most suitable values of the Arc-SAR parameters for each application. As an example, Figure 4 shows the range and cross-range resolutions (ΔR and $\Delta x = R \cdot \Delta \theta$) obtained as a function of the radius of rotation of the antenna and the
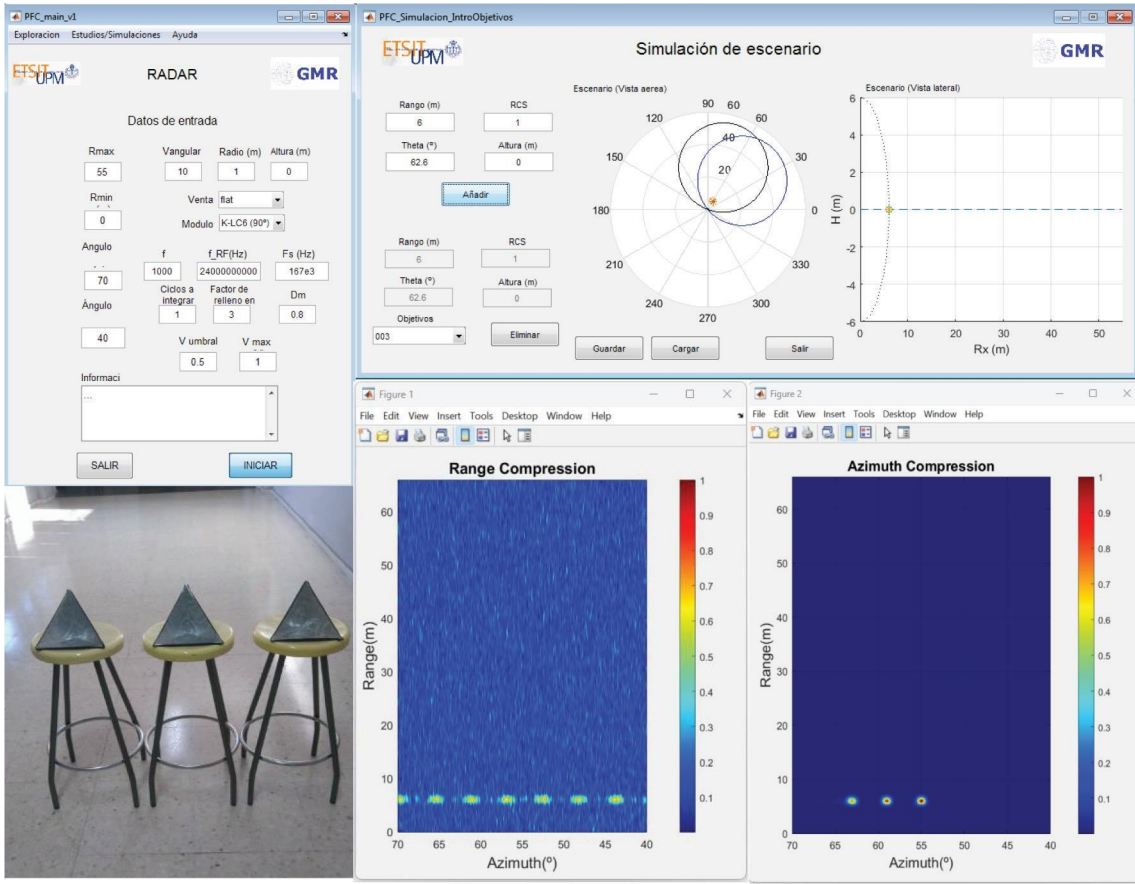
FIGURE 2: Simulation programs: user interface and intermediate results.
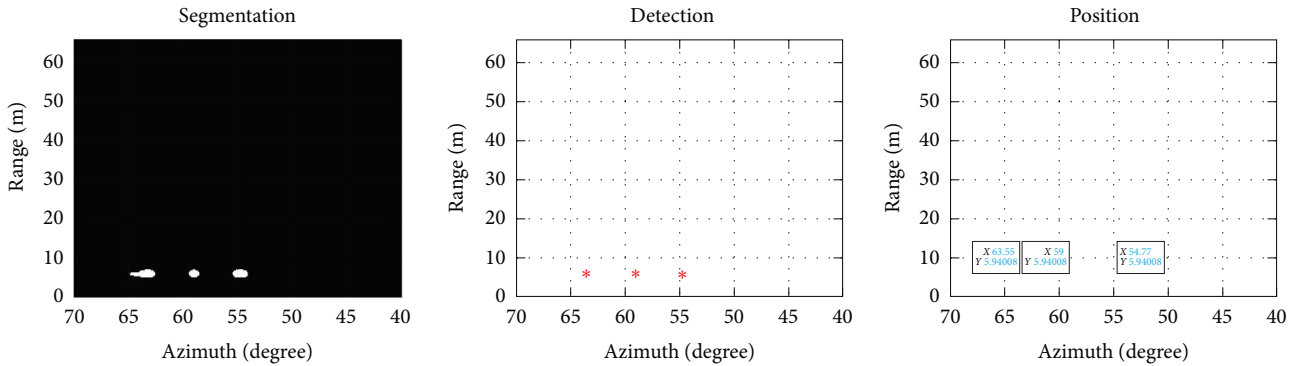
FIGURE 3: Obtaining the images, segmentation, and calculation of the position of the targets.

distance to the target when the range and azimuth migration corrections are not applied and the transmitted bandwidth is 181.5 MHz. The resolution has been set to half of the maximum value.

Note that, effectively as the antenna's turning radius is increased, the resolution of the target improves. However, azimuthal migration degrades the resolution, which worsens more as the target gets closer but it is not significant in terms of cross range. In this case, $L \approx 1$ m will be a good value because the range and cross-range resolutions are equal to the distance of 300 m, maximum prototype range.

Figure 5 shows the azimuthal errors obtained for a point target as a function of the SNR and are compared with those obtained in a monopulse system that uses different antenna apertures and works in the same conditions, specifically with the following parameters:

(1) Central frequency: 24 GHz

(2) Transmitted bandwidth: 181.5 MHz

(3) Pulse repetition frequency (PRF): 1,000 pulses per second (pps)

(4) Azimuth beam width of the antenna: 80°
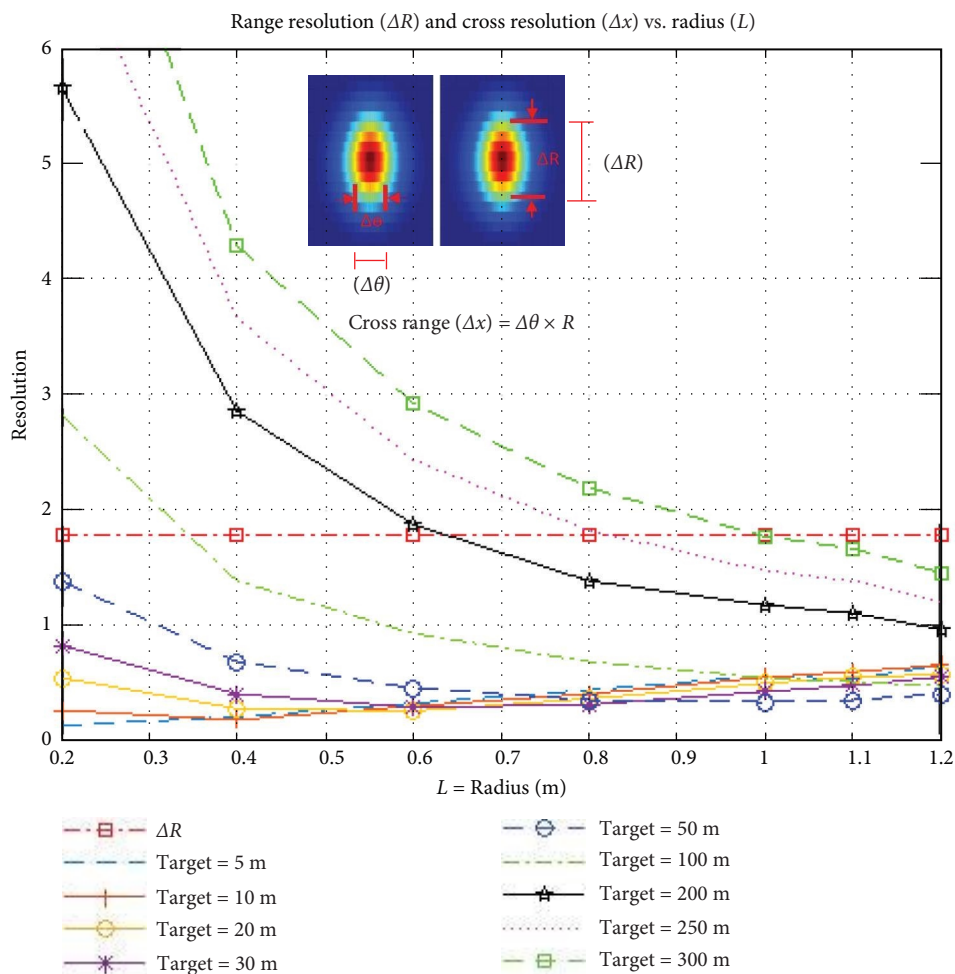
FIGURE 4: Range resolution and azimuth resolution vs. radius.

(a)

(b)
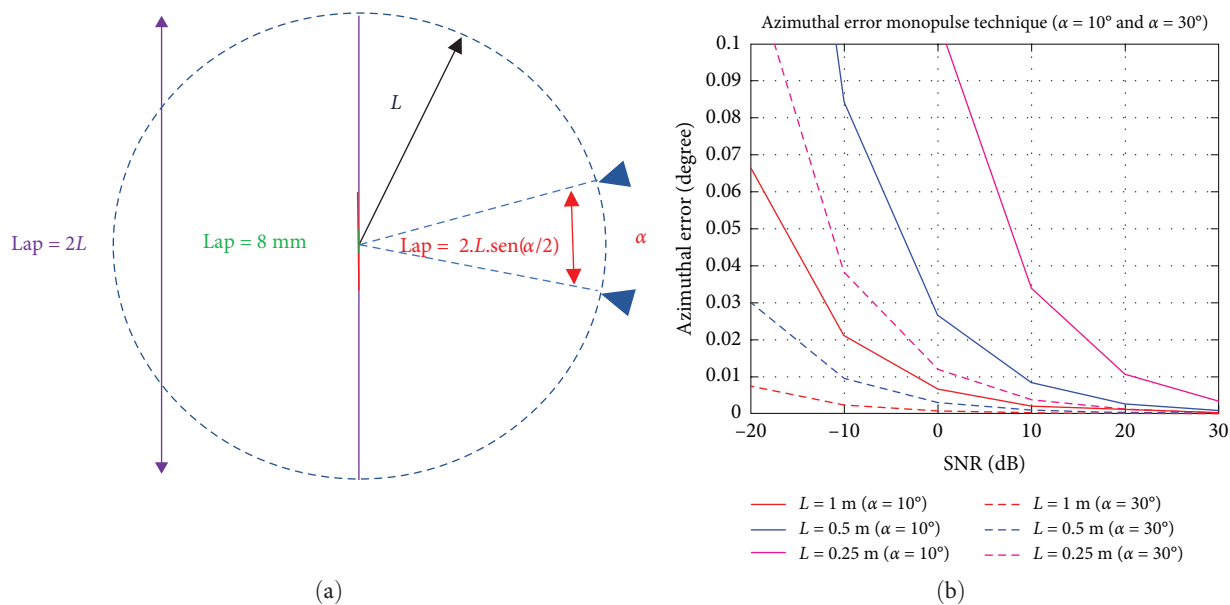
FIGURE 5: Continued.

(c)
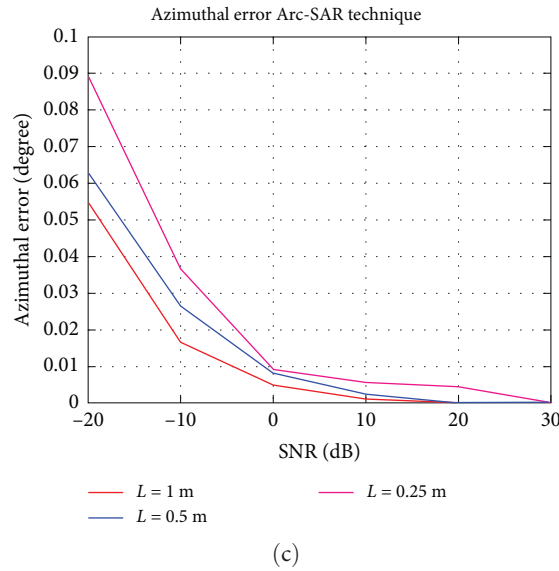
FIGURE 5: (a) Monopulse technique geometry. (b) Azimuthal errors based on the SNR monopulse technique. (c) Azimuthal errors based on the SNR Arc-SAR technique.
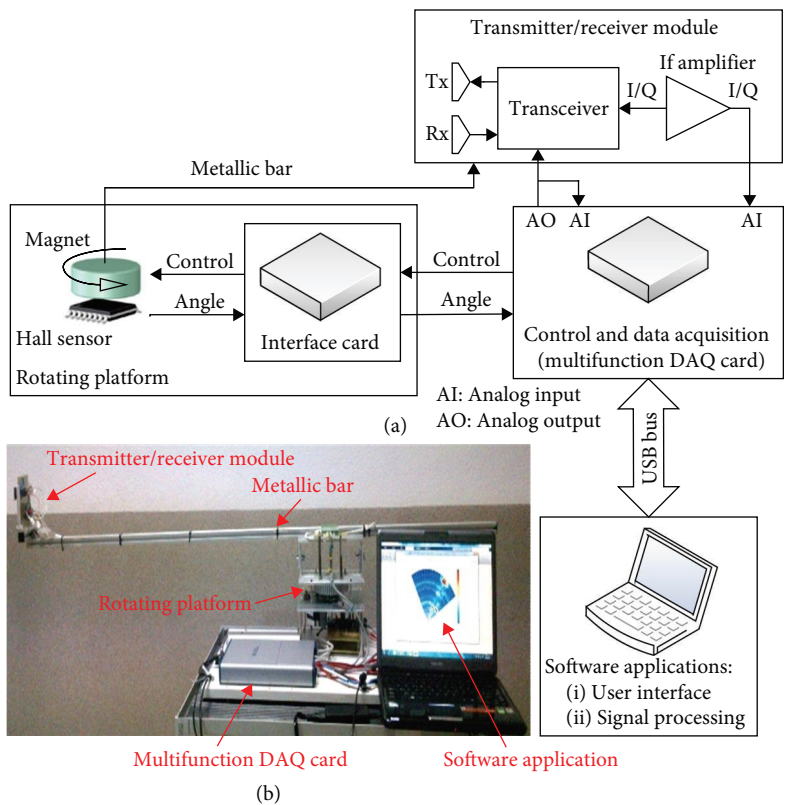
FIGURE 6: (a) FMCW Arc-SAR prototype block diagram. (b) Photograph of the system.

(5) Scanning sector: 30°

(6) Scan speed: 10°/s

(7) Sampling frequency: 166.7 KSamples/s

It can be seen that the results presented in Figure 5 allow us to state that a monopulse system requires a system of antennas with an aperture similar to that synthesized with an Arc-SAR to achieve approximately the same precision, which implies much greater volume, weight, and size of the system. These results were obtained through our simulator because it is very difficult to estimate them experimentally.
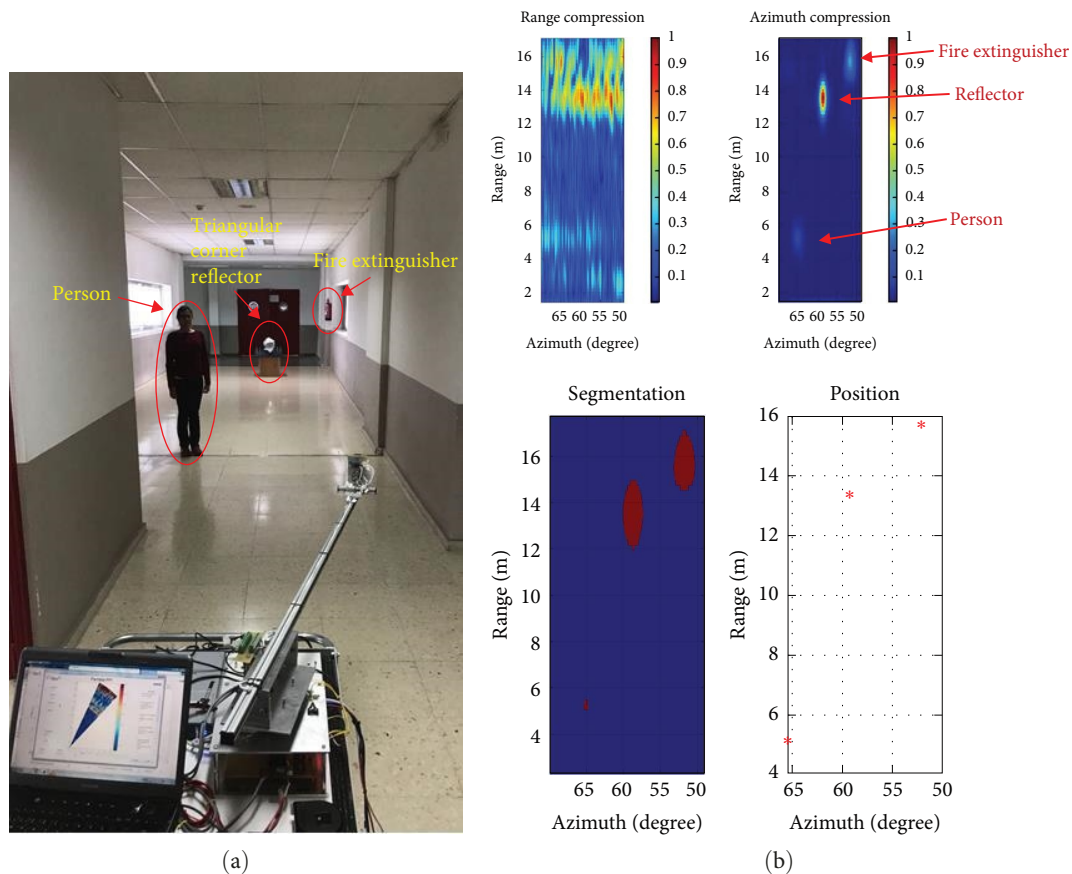
FIGURE 7: First experimental environment. (a) Scene where the experimental measurements have been carried out. (b) Arc-SAR images with the accurate location of the targets.

TABLE 1: First experiment: comparison between the real locations and the measured locations of the targets.

Target	Real range (m)	Real azimuth	Measured range (m)	Measured azimuth
1 (Person)	5.6	6°	5.165	6.12°
2 (Triangular corner reflector)	13.2	0°	13.34	0°
3 (Fire extinguisher)	15.3	−7.12°	15.71	−7.21°

5. Experimental Prototype of an Arc-SAR System

A short-range (up to 250 m) FMCW radar system, synthetic aperture with rotational movement of the antennas, in K-band (operates at 24 GHz), has been developed for the realization of experiments quickly and easily. Figure 6 shows the block diagram and a photograph of the system. For its implementation, common commercial elements have been selected, @as far as possible. Among them, we can highlight the low-cost transceiver module K-LC6, manufactured by RF beam Microwave GmbH, which integrates all radio-frequency elements: the antennas, the transmitter, and the receiver. Another important element of the system is the multifunction data acquisition card (DAQ), also low-cost, which is programed through MATLAB^{M}, and allows the generation and acquisition of signals in a synchronized manner, among other functions.

The prototype is endowed with great flexibility in its operation, allowing the modification of its operational parameters and the inclusion of all kinds of algorithms to compute the output signals of the transceiver.

6. Experimental Results

Several experiments have been carried out, demonstrating the performance of the system. In this article some of them are presented. All of them have been made with a turning radius of 1 m.

In the first experiment there is a person and a triangular corner reflector which simulates another radar target. The results obtained are presented in Figure 7 and in Table 1. Note that the targets are detected and located with great precision, even a fire extinguisher located near the triangular corner reflector is detected and located to the right of the scene. The errors in range are due to the distance discretization
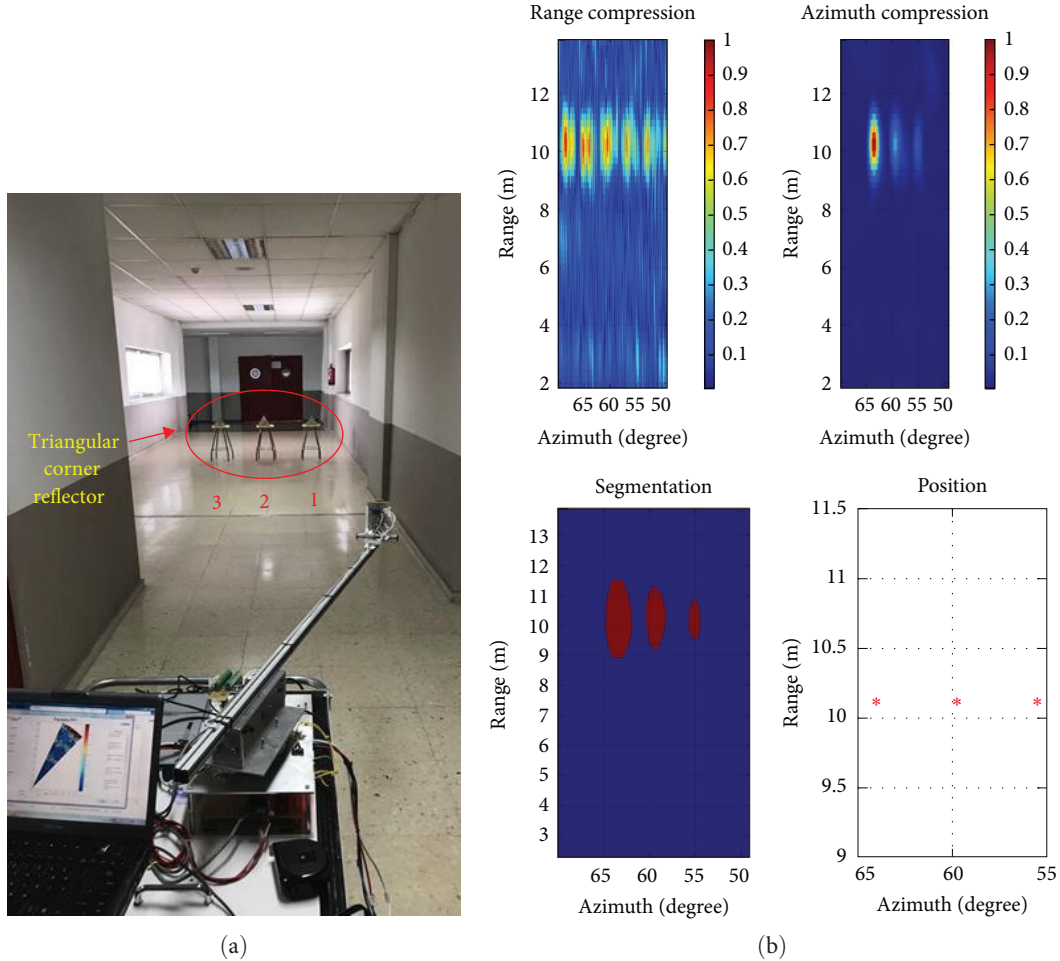
FIGURE 8: Second experimental environment. (a) Scene where the experimental measurements have been carried out. (b) Arc-SAR images with the accurate location of the targets.

TABLE 2: Second experiment: comparison between the real locations and the measured locations of the targets.

Target	Real range (m)	Real azimuth	Measured range (m)	Measured azimuth
1	10	−4.28°	10.12	−4.22°
2	10	0	10.12	0°
3	10	4.28°	10.12	4.21°

used (approximately 0.5 m). The azimuth errors are around 0.1°, which would mean a cross-range error of less than 3 cm for the farthest target in this scene (the fire extinguisher) and approximately 0.5 m for targets at 300 m (maximum expected radar range), since this angular error remains constant with distance if the SNR is sufficiently high throughout the coverage area. Note that, as expected, the range and azimuth accuracy errors are lower than the range and azimuth resolutions shown in Figure 4.

In the second experiment, three triangular corner reflectors have been placed at the same distance. In this case the signals reflected by the targets are combined in the same range resolution cell. Figure 8 and Table 2 show the experimental results obtained, which are similar to those of the

previous case and demonstrate the extraordinary precision of an Arc-SAR system. Note that, the reflectors have different radar sections because of their different alignment with the radar but the radar is able to distinguish each of the targets, and locates them in a very precise way. The fact that the range errors are constant indicates that this is an error associated with the range resolution of the system, as already indicated in the interpretation of the first experiment. It is also found that the azimuth errors are less than 0.1°, which at this distance corresponds to a cross-range error of approximately 1 cm.

Obviously, to be able to detect and locate the targets it is necessary that the system be able to distinguish each of the targets. Figures 9 and 10 present the results obtained when
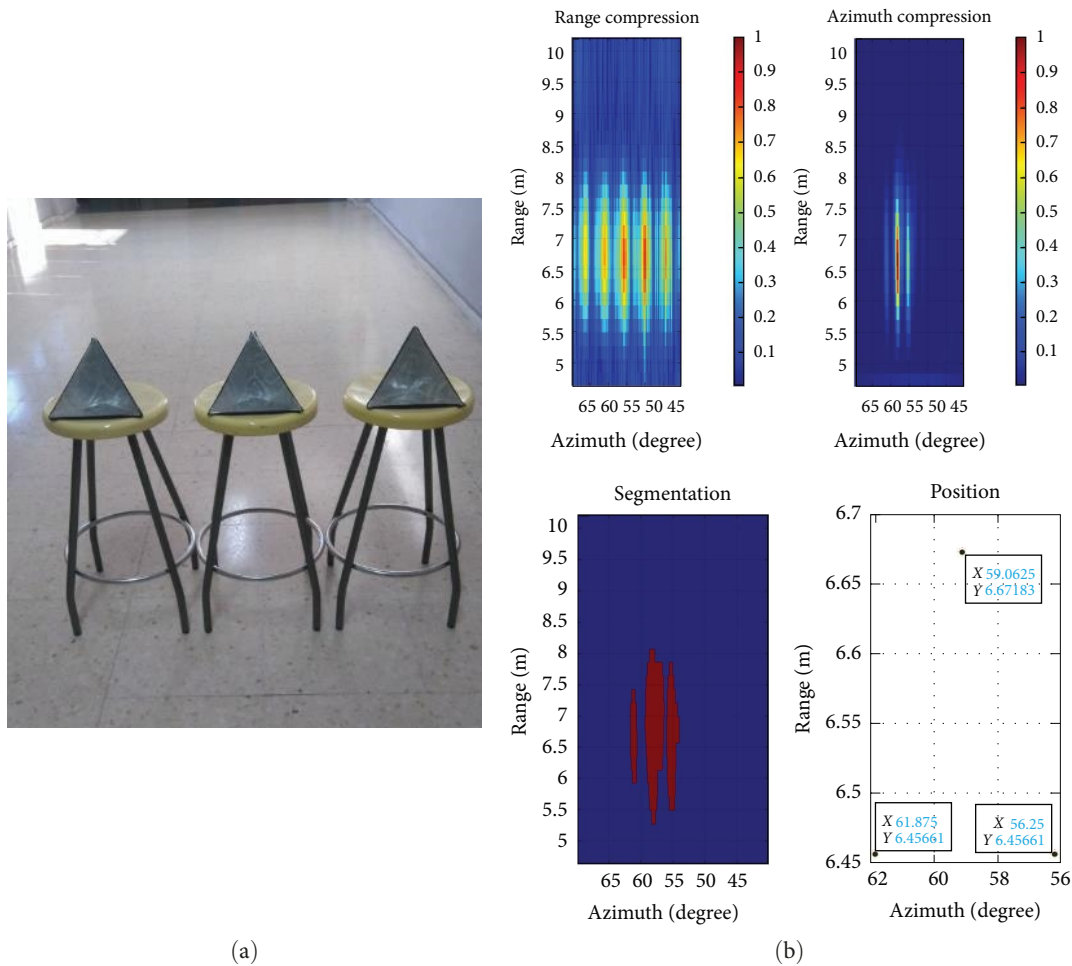
FIGURE 9: Third experimental environment. (a) Scene where the experimental measurements have been carried out. (b) Arc-SAR images with the accurate location of the targets.

the reflectors are very close. The size of the reflectors prevents them from being closer together, and the reflectors are not exactly point targets, which degrades the measured azimuthal resolution capability. The simulation software does not have these restrictions and shows that targets can be distinguished each other at a distance of 300 m with range and cross-range separations of less than 2 m, decreasing (i.e., improving) proportionally to several centimeters for distances of less than 10 m. The values obtained by simulation are consistent with those observed in the experimental results.

7. Discussion

The experimental results support the theoretical results obtained using the developed software tool and validate the possibilities of the proposed technique. Both results confirm other previously published results such as the dependency of the obtained features on the synthesized aperture, specifically on the size of the antenna and the beam width, and in addition to the effects of the range and azimuth migrations and its dependency on the distance to the target. The both migrations can be compensated but this requires an enormous computational effort.

This work concludes that the precision of an Arc-SAR is similar to that obtained with a radar that uses a monopulse system and an antenna with an aperture similar to that synthesized in the first one. The monopulse antenna would have much larger size, weight, and cost, which carries a greater difficulty to install in small aerial platforms.

The future line of investigation will be oriented toward studying the possibility of installing the Arc-SAR in small drones capable of performing the antenna's turn using their own flying systems.

8. Conclusions

In the previous sections, the possibility of using an Arc-SAR technique to obtain radar images and highly accurate target location, using small-sized and light-weight antennas has been demonstrated, both theoretically and experimentally.

To this end, a simulator of the behavior of these systems in complex environments has been developed and a complete prototype has been implemented to verify the possibilities and limitations of this technique.

The simulator, in addition to the allowing parametric analysis, can be used to design an Arc-SAR, by selecting the
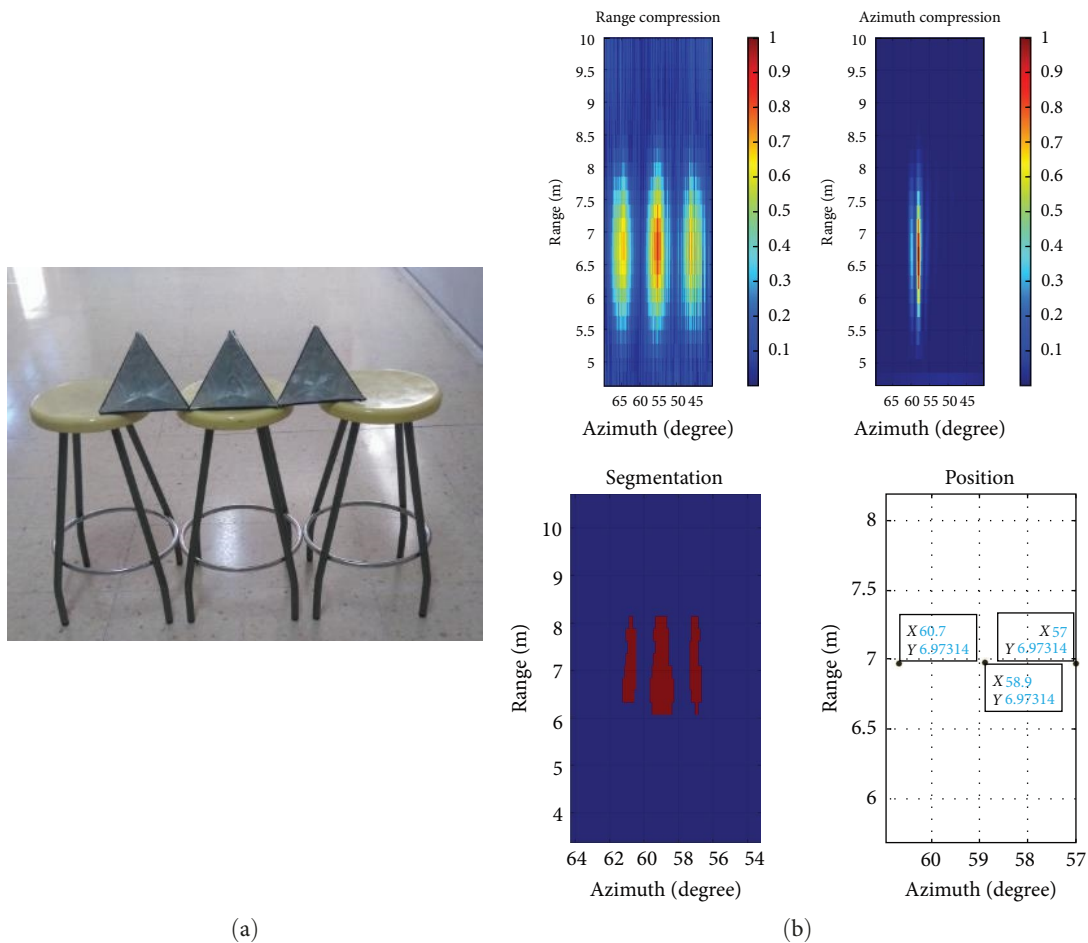
FIGURE 10: Forth experimental environment. (a) Scene where the experimental measurements have been carried out. (b) Arc-SAR images with the accurate location of the targets.

most appropriate values for its parameters in each application. The data obtained allow us to consider its application in high-reach weapon systems (to estimate the initial position of the target to which a self-guided weapon is launched) or for short and medium ranges using directly the obtained position.

A particularly interesting case of application is when the radar is shipped aboard aerial platforms (such as RPAS: remotely piloted aircraft systems), which can easily generate circular movements (e.g., quadcopters) or have rotating elements such as helicopters. In any case, you can always obtain a reduction in volume, weight, and cost (always interesting on an on-board radar) that will have a much more complex signal processing as counterpart, but it is already within the reach of the available digital technology.

Data Availability

No underlying data were collected or produced in this study.

Consent

The participants accepted for this experiment and informed consent was obtained from the individual participants included in the study.

Conflicts of Interest

The authors declare that there is no conflicts of interest regarding the publication of this paper.

References

[1] S. M. Sherman and D. K. Barton, *Monopulse Principles and Techniques*, Artech House, 2nd edition, 2011.

[2] A. Moreira, P. Prats-Iraola, M. Younis, G. Krieger, I. Hajnsek, and K. P. Papathanassiou, "A tutorial on synthetic aperture radar," *IEEE Geoscience and Remote Sensing Magazine*, vol. 1, no. 1, pp. 6–43, 2013.

[3] M. Pieraccini and L. Miccinesi, "ArcSAR: theory, simulations, and experimental verification," *IEEE Transactions on Microwave Theory and Techniques*, vol. 65, no. 1, pp. 293–301, 2017.

[4] H. Klausing, N. Bartsch, and C. Boesswetter, "A MM-wave SAR-design for helicopter application (ROSAR)," in *1986 16th European Microwave Conference*, pp. 317–328, IEEE, Dublin, Ireland, September 1986.

[5] H. Klausing and W. Keydel, "Feasibility of a synthetic aperture radar with rotating antennas (ROSAR)," in *IEEE International Conference on Radar*, pp. 51–56, IEEE, Arlington, VA, USA, May 1990.

[6] M. Mohammadpoor, R. S. A. Raja Abdullah, A. Ismail, and A. F. Abas, "A circular synthetic aperture radar for on-the-ground object detection," *Progress In Electromagnetics Research*, vol. 122, pp. 269–292, 2012.

[7] Y. Luo, H. Song, R. Wang, Y. Deng, F. Zhao, and Z. Xu, "Arc FMCW SAR and applications in ground monitoring," *IEEE Transactions on Geoscience and Remote Sensing*, vol. 52, no. 9, pp. 5989–5998, 2014.

[8] F. Ali, G. Bauer, and M. Vossiek, "A rotating synthetic aperture radar imaging concept for robot navigation," *IEEE Transactions on Microwave Theory and Techniques*, vol. 62, no. 7, pp. 1545–1553, 2014.

[9] H. Lee, J.-H. Lee, K.-E. Kim, N.-H. Sung, and S.-J. Cho, "Development of a truck-mounted arc-scanning synthetic aperture radar," *IEEE Transactions on Geoscience and Remote Sensing*, vol. 52, no. 5, pp. 2773–2779, 2014.

[10] D. Li, H. Liu, Y. Liao, and X. Gui, "A novel helicopter-borne rotating SAR imaging model and algorithm based on inverse chirp-Z transform using frequency-modulated continuous wave," *IEEE Geoscience and Remote Sensing Letters*, vol. 12, no. 8, pp. 1625–1629, 2015.

[11] W.-J. Li, G. Liao, S. Zhu, and J. Xu, "A novel helicopter-borne RoSAR imaging algorithm based on the azimuth chirp z transform," *IEEE Geoscience and Remote Sensing Letters*, vol. 16, no. 2, pp. 226–230, 2019.

[12] Y. Wang, Y. Song, Y. Lin, Y. Li, Y. Zhang, and W. Hong, "Interferometric DEM-assisted high precision imaging method for ArcSAR," *Sensors*, vol. 19, no. 13, Article ID 2921, 2019.

[13] Y. Lin, Y. Song, Y. Wang, and Y. Li, "The large field of view fast imaging algorithm for arc synthetic aperture radar," *Signal Process*, vol. 35, pp. 499–506, 2019.

[14] M. Qin, D. Li, X. Tang, C. Zeng, W. Li, and L. Xu, "A fast high-resolution imaging algorithm for helicopter-borne rotating array SAR based on 2-D chirp-Z transform," *Remote Sensing*, vol. 11, no. 14, Article ID 1669, 2019.

[15] Y. Wang, Q. Song, J. Wang, and H. Yu, "Airport runway foreign object debris detection system based on arc-scanning SAR technology," *IEEE Transactions on Geoscience and Remote Sensing*, vol. 60, pp. 1–16, 2022.

[16] H. Wang, B. Sun, C. Li, Y. Jiang, and W. Yang, "An improved range-doppler imaging algorithm based on high-order range model for near-field panoramic millimeter wave ArcSAR," *IEEE Transactions on Geoscience and Remote Sensing*, vol. 61, pp. 1–16, 2023.

[17] F.-J. Romero-Paisano, F. Pérez-Martínez, S. Martínez-Cordero, and J. Calvo-Gallego, "Accurate multi-target surveillance system over wide areas," in *2017 International Carnahan Conference on Security Technology (ICCST)*, pp. 1–6, IEEE, Madrid, Spain, 2017.

[18] D. K. Barton, *Handbook of Radar Measurement*, Artech House, 1984.

[19] B. R. Mahafza and A. Z. Elsherbeni, *MATLAB: Simulations for Radar Systems Desing*, CHAPMAN &HALL/CRC, 2004.

[20] Y. He, T. Hu, and D. Zeng, "Scan-Flood Fill (SCAFF): an efficient automatic precise region filling algorithm for complicated regions," in *2019 IEEE/CVF Conference on Computer Vision and Pattern Recognition Workshops (CVPRW)*, pp. 761–769, IEEE, Long Beach, CA, USA, June 2019.